

## Shear Layer and Wave Structure Over Partially Spanning Cavities

Rajarshi Das\*, Heuy Dong Kim\*<sup>+</sup> and Job Kurian\*\*

**Abstract.** Study of the wave structure and shear layer in the vicinity of a wall mounted cavity is done by time averaged colour schlieren and time resolved instantaneous shadowgraph technique in an  $M=1.7$  flowfield. Effect of change of cavity width on flow structure is investigated by using constant length to depth ( $L/D$ ) ratio cavity models with varying length to width ( $L/W$ ) ratio of 0.83 to 4. The time averaged shock wave structure was observed to change with change in cavity width. Dependence of the shock angle at the leading edge on the shear layer width is also evident from the images obtained. Unsteadiness in the flow field in terms of shear layer dynamics and quasi steady nature of shock waves was evident from the images obtained during instantaneous shadowgraph experiments. Apart from the leading and trailing edge shocks, several other waves and flow features were observed. These flow features and the associated physical phenomena are discussed in details and presented in the paper.

**Key Words:** Partial span cavity, Shock, Wave, Shear Layer

### 1. INTRODUCTION

Flow over cavities under various conditions has been widely investigated to gain an insight into the underlying physical aspects of the allied complex nature of flow behavior. The flow is characterized by pressure oscillations, generation of unsteady waves and shear layer structure, vortices and mass exchange between cavity and freestream.

Schematic diagram of a cavity over which flow is taking place is shown in Fig.1 where  $L$  denotes the length of the cavity and  $D$  its depth. The incoming boundary layer separates at the leading edge of the cavity. This transforms into a free shear layer and interacts with the trailing edge, depending on various geometric and fluid dynamic aspects. The shear layer behaviour governs the different flow features exhibited in the vicinity of the cavity. Generation of periodic pressure oscillations, various waves in the flow field

and dynamics of the free shear layer are the basic features for such flows.

However, when the primary flow field is supersonic, several other flow features develop. These features depend on the cavity geometry, mainly on its  $L/D$  ratio. Investigators have classified cavities as open, closed and transitional depending on these flow features<sup>1,2)</sup>

The commonly accepted classification of cavities is as follows:

(a) Open cavity: When the separated shear layer reattaches at the trailing edge of the cavity, spanning its entire length then it is called open cavity. This phenomenon is observed when cavity  $L/D$  is less than 7~8.

(b) Closed cavity: When the separated shear layer reattaches at the bottom of the cavity, then it is called closed. This is observed when cavity  $L/D$  is greater than 13. A schematic of flow field over the cavities with different  $L/D$  ratio is shown in Figure 2.

The flapping motion of the shear layer above the cavity is generated by the periodic pressure difference between the cavity and the mainstream flow. As the pressure inside the cavity increases, the shear layer comes out of the cavity and creates an obstruction to

---

<sup>+</sup> Andong National University

E-mail: kimhd@andong.ac.kr

\* Andong National University

\*\* Indian Institute of Technology Madras

the incoming supersonic flow at the cavity leading edge. This generates an oblique shock wave at the leading edge of the cavity in the primary flowfield. As the shear layer comes out of the cavity, fluid is ejected near the cavity trailing edge, thereby decreasing the pressure inside the cavity. This causes the shear layer to dive back into the cavity, exposing the trailing edge to create an obstruction to the primary supersonic flow. As the supersonic flow experiences this, a bow shock is generated in the vicinity of the trailing edge. This basic wave structure generation mechanism becomes all the more complex with the acoustic waves traveling inside the cavities because of the supersonic fluid hitting the trailing edge and the vortices in the shear layer interacting with the cavity trailing edge wall. A coupled mechanism of this phenomenon is discussed in detail later in the paper

Unlike the extensive work done on the effect of  $L/D$  ratio of cavity on the flow physics, reports on study of effect of cavity width on the flow characteristics has been lacking in available literature. Investigations on the effect of cavity width mostly reported three dimensionality of flow structure. But these works are limited to two dimensional cavities (cavities which span the entire width of the test section) only with very few researchers reporting studies on actual three dimensional cavities (partially spanning cavities). Cavities which span the width of the test section only partially are designated in this paper as 3D cavities. The classification between two dimensional and three dimensional cavities is illustrated in Fig.3 which shows the planform of the test section.

This paper presents a detailed study of both time averaged and time resolved flow features of flow over partially spanning cavities of varying width. Cavities

with different widths were used for the study thereby giving  $L/W$  ratios of 0.83 to 4. The cavity with  $L/W$  ratio of 0.83 spans the entire width of the test section which is equivalent to a 2D cavity. The other cavities are of less width and are of the partially spanning type. All the cavities are located axi-symmetric with the test section.

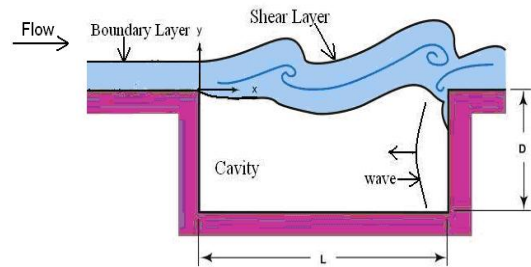


Fig.1. Schematic of flow over a cavity

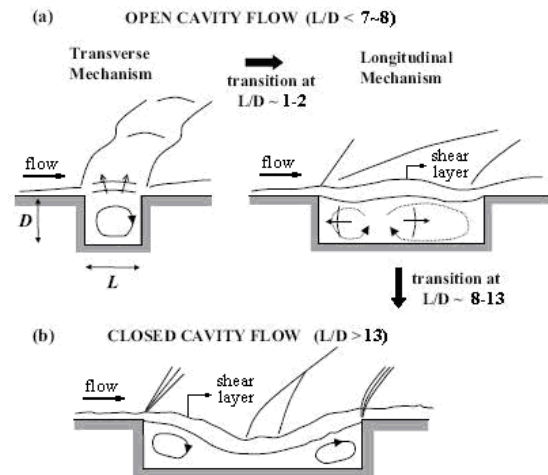


Fig. 2. Cavity classification based on shear layer features

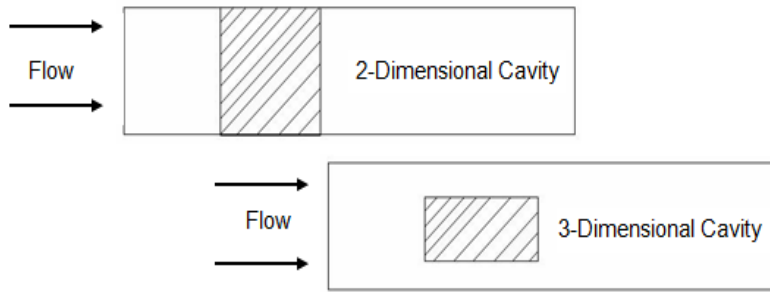


Fig. 3. Schematic of 2D cavity and 3D cavity along the floor of flow passage

## 2. EXPERIMENTAL SETUP

A supersonic freejet facility was used for the experiments. A convergent-divergent (c-d) nozzle and test section were designed and fabricated for the current work. The supersonic flow at Mach no. of 1.7 is obtained by coupling a settling chamber and a c-d nozzle to one of the distribution pipe lines coming from the air reservoirs. Stagnation pressure of the incoming flow is measured in the settling chamber using a Bourdon gauge. The c-d nozzle is designed such that its top and bottom surfaces are convergent-divergent while the sides are parallel to each other. The divergent part of the c-d nozzle expands to a rectangular cross section of 30 mm height and 60 mm width, which is same as the cross section of the test section.

The test-section is a rectangular duct with a wall mounted cavity on the bottom wall. Separate models were fabricated for each of the test cases. The top and bottom walls are made of perspex. The side walls are made of clear float glass of 8 mm thickness. The Mach 1.7 flow is maintained in the test section of cross section 60x30mm<sup>2</sup> at a flow Reynolds number of 1.1805e06 based on the cavity length. Cavities of length 50mm and depth 25mm were used for the study. The cavities are placed 50mm downstream of nozzle exit. Width of the 3D cavities were kept at 25mm, 16.7mm and 12.5mm in different sets of experiments thereby giving L/W ratios of 2, 3 and 4 for the three cases. The

L/D ratio of the cavity was kept constant at 2.0 for all the cases. The 2D cavity of the same length (50mm) and depth (25mm) used for the study spanned the entire width of 60mm of the test section and was of L/W ratio of 0.83. A 3D isometric view of the test section is shown in Fig.4.

The setup for colour schlieren visualization consists of two concave mirrors, light source, pinhole, prism, knife-edge, screen and digital camera as shown in Fig.5. The collimating mirrors are arranged on either side of the test section. White light from a 50W tungsten-halogen light source (Newport make) is used as the source. The light emerging from the pinhole is incident on a dispersion prism, to split the light into its constituent colours. This dispersed light collimated by one of the mirrors passes through the test section onto the other mirror. The knife edge is placed at the focus of the second concave mirror. The knife edge is adjusted so that green is made the background colour. The density gradient across the test section, deflects the light and gives rise to different colours, depending on whether the gradient is positive (compression) or negative (expansion). The resultant

image is captured using the digital camera. The camera used is Olympus Camedia SLR Digital camera (model E 20) of five mega-pixel resolution and one second exposure time.

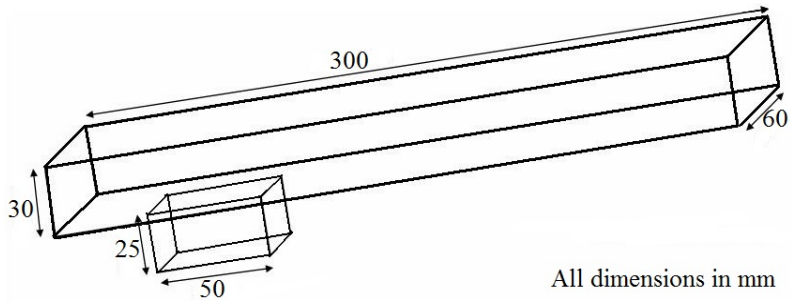


Fig. 4. Schematic diagram of 3D cavity configuration

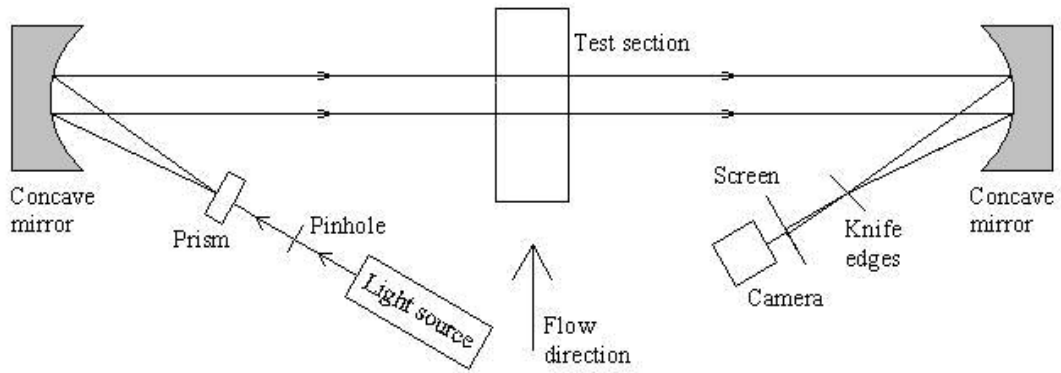


Fig. 5. Schematic of colour schlieren setup

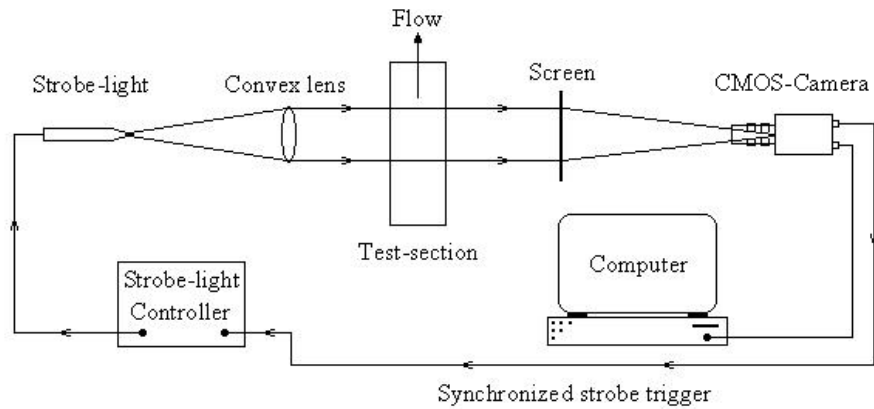


Fig. 6. Schematic of instantaneous shadowgraph setup

Instantaneous shadowgraph imaging is done to study the transient nature of the flow in the vicinity of the cavity. The experimental setup of shadowgraph visualization is shown schematically in Fig.6. The light source used is Nanolite™ spark light system controlled by Strobokin™ generator which generates trains of sparks with controllable frequency. In each pulse, light-strobe produces 25 mV of energy in 18 ns time at a maximum flashing rate of 20 kHz. The light from the strobe source is collimated using a convex lens of 10cm diameter and 20 cm focal length.

The collimated light beam is passed through the area of interest in the test-section and made to fall on the screen. The camera used to capture the image is a high-speed CMOS-camera of Redlake make, model N-4. The camera at full resolution of 1024x1024 pixels can go up to 4000 frames per second (fps) in plus mode, and has an image depth of 10-bit mono and 30-bit color. The camera has a minimum exposure time of 1  $\mu$ s, and is software triggered and controlled using a computer. Strobe-light of 18 ns duration is synchronized with the camera using a low noise BNC connector, as shown in the Fig.6. The camera is triggered internally using the control software. The strobe light is triggered by an external pulse from the camera. For all the models tested in the present work, the images of the unsteady flow over the cavities are taken at 1500 fps at full pixel resolution.

### 3. EXPERIMENTAL RESULTS

Schlieren flow visualization gives qualitative information about the flow field around the cavities. It captures the density gradients and hence can give information regarding the shear-layer and the cavity leading and trailing-edge shock patterns. For obtaining better resolution of the density variations, colour schlieren technique is used in the present study. The white light is dispersed using a prism into 'VIBGYOR' with violet colour having the highest refractive index which reduces towards the red colour. The test-section background is maintained as green during the no-flow condition. In the schlieren pictures, blue, indigo and

violet colours show higher density or compression regions whereas yellow, orange and red show expansion regions. The camera used for imaging had an exposure time of 1sec which averages the flow features over a time period of one second.

Images obtained during schlieren visualization are shown in Fig.7. The flow direction is from left-to-right of the page. Steep density gradients are observed at the leading and trailing edges of all the cavities. Unsteady movement of the shear layer in the vertical direction downstream of the leading edge creates obstruction to the freestream supersonic flow and hence oblique shocks are formed. The flapping of the shear layer at the trailing edge causes the exposure of the edge to supersonic freestream flow thus generating a detached bow shock at the trailing edge.

Difference in the shear layer thickness at the leading edge is apparent from the images obtained for models of  $L/W=2$  and  $L/W=4$ . For the  $L/W=2$  model, the shear layer is observed to grow in thickness rapidly near the cavity lip just after the leading edge shock. Thickness of the shear layer for the  $L/W=4$  cavity is less as compared to the cavity of  $L/W=2$ . The nature of acoustic disturbance near the leading edge may have a direct impact on the thickness of the shear layer. Acoustic disturbance has been observed to be of much higher amplitude for the cavity of  $L/W=2$ . This high amplitude oscillation perturbs the shear layer at the leading edge causing it to deflect into the mainstream flow. The obstruction created in the mainstream flow by the deflected shear layer generates the leading edge shock. As the structure of the shear layer at the leading edge is observed to be different for each case, the amplitude of the oscillation seems to play an important role in the flow physics associated with the models.

According to the physical phenomena associated with supersonic flow over cavities the free shear layer at the leading edge of the cavity is perturbed by the acoustic wave moving inside the cavity which causes vortex shedding and creates a feedback loop for the self sustaining oscillations within the cavity. The flapping movement of the shear layer normal to the flow direction is associated with periodic inflow and outflow

of mass from the cavity due to this. This also affects the leading and trailing edge shock, making them highly unsteady in nature. Thus, both the shocks exhibit quasi-steady characteristics. As the shear layer protrudes outside the cavity at the leading edge, the leading edge shock can be seen. As the shear layer dives back into the cavity at the leading edge an expansion fan is formed in the location. This quasi-steady nature of the leading edge shock is manifested in the colour variation along the axial direction of the test section.

According to Gladstone Dale's equation, the refractive index gradient varies in similar nature as the density gradient. For an expansion wave, a negative density gradient exists in the flowfield and this is visible as yellow, orange and red in the colour schlieren images. Due to quasi-steady nature of expansion fan at the leading edge of the cavity, a similar region is observed in the flow adjacent to the leading edge shock for some of the models. This region shows the imprint of an expansion wave which occurs every time the shear layer dives into the cavity and the freestream flow experiences an expansion corner aft of the leading edge.

Thickness of the shear layer at the leading edge in turn affects the shock angle at the leading edge. The shock angle is observed to be higher for the  $L/W=2$  cavity than the other two 3D models and the 2D model. The trailing edge shock angle is observed to be same in all the cases implying that the trailing edge is exposed to identical freestream conditions for all the cavities. A region of high density gradient is observed at the bottom corner of trailing edge wall for the narrower cavities. This could be due to the movement of the vortical structures along the trailing edge and along the floor following the circulation present at the trailing edge. Similar observation was made also by Zhang<sup>3)</sup>.

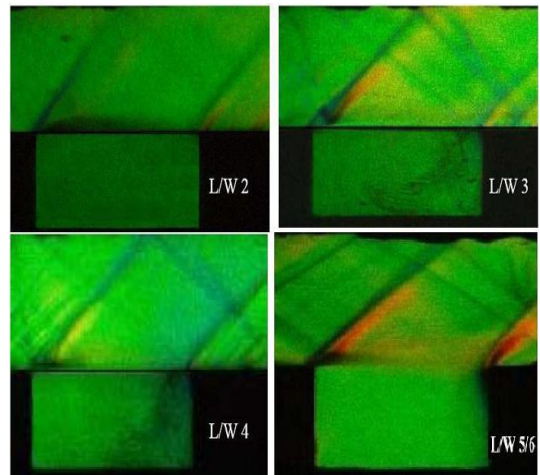


Fig. 7. Time averaged schlieren images

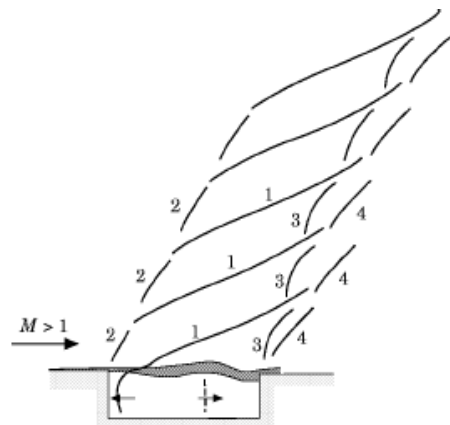


Fig. 8. Wave structure for supersonic flow past cavities<sup>4)</sup>

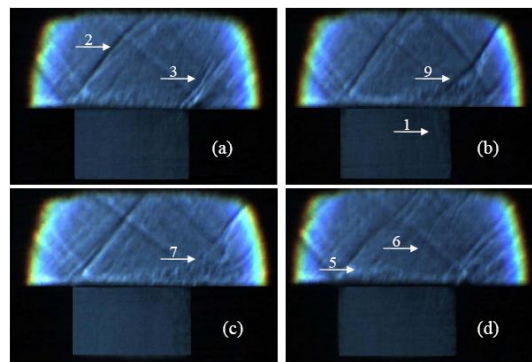


Fig. 9. Instantaneous shadowgraph images of flow over cavity with  $L/W=2$

Instantaneous flow visualization is performed to study the unsteady nature of flow past cavities. Wave structure of supersonic flow past cavities has been explained by many previous researchers<sup>4,5</sup>. The illustration of the wave structure shown in Fig.8 is by Heller and Delfs<sup>4</sup>.

In Fig.8, wave 1 depicts the upstream moving acoustic wave inside the cavity and its projection in the mainstream. When the externally trailed front reaches the leading edge it detaches from the cavity internal stem and swims off into the external medium. A quasi-steady compression wave appears each time the shear layer is deflected upwards at the leading edge. This wave is shown in Fig.8 as wave 2. Each time the shear layer dives into the cavity the trailing edge is exposed to the supersonic freestream. This results in the appearance of a bow shock shown as wave 3 in Fig.8. During the upward motion of the shear layer at the trailing edge and its subsequent reattachment at the surface just beyond the trailing edge a compression wave shown as wave 4 occurs.

Cavities that excite discrete oscillations exhibit distinct features like leading and trailing edge shock, waves traveling inside the cavities and their projection in the mainstream flow, vortex roll up and shock waves associated with unsteady shear layer. Periodic nature of these unsteady oscillations enables presentation of the associated flow features as sequential images obtained during instantaneous shadowgraph visualization.

Different waves and flow structure occurring in the vicinity of the 3D cavity with L/W ratio 2 is shown in Fig.9 (a)-(d). The flow direction is from left to right of the page. Apart from the features already discussed with reference to Fig.8, some additional observations were made which are described subsequently. Images were acquired at a rate of 1500fps. Strong shock in the mainstream is observed at the leading edge of the cavity due to deflection of shear layer as marked by wave 2.

As the shear layer starts diving into the cavity at the trailing edge, a bow shock appears as wave 3 in Fig.9(a), and the shear layer is observed to impinge on the trailing edge. A compression wave (1) is produced due to the impingement which travels in the upstream

direction inside the cavity. Projection of this wave is noticed in the mainstream near the trailing edge in Fig.9(b). This wave immediately disturbs the shear layer in the vicinity of the trailing edge which results in vortex roll up and shear layer coming out near the trailing edge. Multiple waves emanating from the cavity near the trailing edge coalesce to form a lambda shock structure marked as 9 in Fig.9(b). As the shear layer comes out near the trailing edge, exchange of fluid between cavity and mainstream takes place and considerable amount of disturbances is generated in the mainstream marked as structure 7. These disturbances in turn create obstruction to the mainstream supersonic flow and generate bow shocks as seen in Fig.9(d) and marked as 6. As the wave 1 travels inside the cavity it disturbs the shear layer and causes the shear layer to roll up into the mainstream before the leading edge shock is generated.

Similar features were observed for the cavity with L/W ratio 3. Images obtained for this model is shown in Fig.10(a)-(d). The lambda shock structure near the trailing edge of the cavity marked as 9 and the bow shock (6) at half cavity length due to the obstruction caused by upward movement of shear layer are clearly seen in Fig.10(b) and (c). In addition to these features, another prominent wave marked as 8 [Fig.10(d)] was observed during the experiments. Shear layer coming out of the cavity due to upward deflection caused by the moving acoustic wave inside the cavity seemed to be the reason behind generation of this wave.

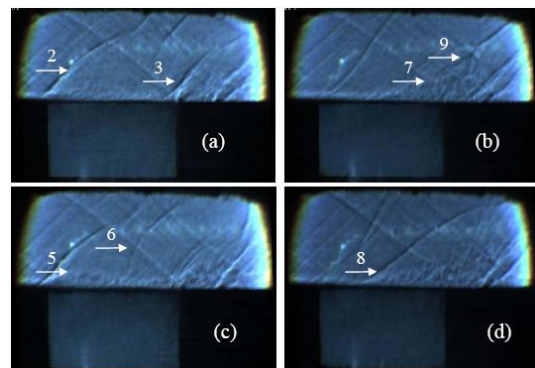


Fig. 10. Instantaneous shadowgraph images of flow over cavity with L/W=3

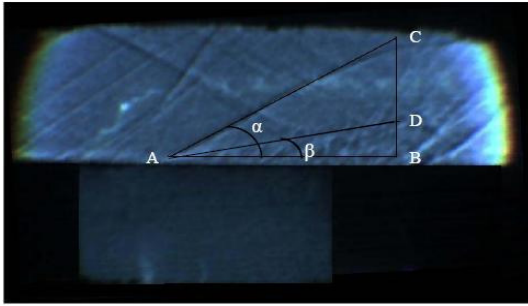


Fig. 11. Instantaneous shadowgraph image of flow over cavity with  $L/W=3$  showing wave 8

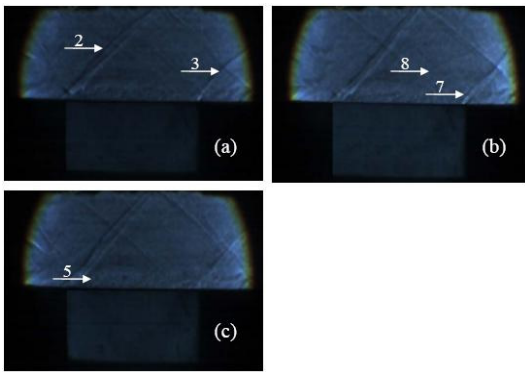


Fig. 12. Instantaneous shadowgraph images of flow over cavity with  $L/W=4$

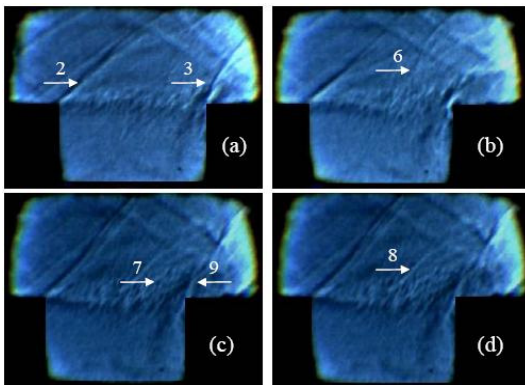


Fig. 13. Instantaneous shadowgraph images of flow over cavity with  $L/W=4$

The wave angle and the shear layer deflection angle with reference to the mainstream flow direction were calculated from the pixel values of the points A, B, C and D for this instantaneous image shown in Fig.11. The maximum shear layer deflection angle  $\beta$  was

obtained as  $9.492^\circ$  and the wave angle  $\alpha$  as  $28.94^\circ$ . Flow Mach number in the vicinity of station A in the mainstream was approximately 1.6234 from the numerical calculations described later in the thesis. For  $M=1.6234$ , and a deflection angle of  $9.492^\circ$ , the actual wave angle is estimated to be much higher than  $28.94^\circ$ . According to the wave structure proposed by Heller and Delfs<sup>4)</sup>, projection of an acoustic wave in the freestream experiences flow at a resultant velocity that is the summation of acoustic velocity at which a disturbance propagates inside the cavity and the freestream supersonic velocity. Thus, for the present study the projected wave experiences a  $M=2.84$  supersonic flow for which the Mach wave angle should be  $20.617^\circ$ . But the wave angle  $\alpha$  observed in Fig.11 is  $28.94^\circ$  which is higher than the Mach wave angle. Again, for a supersonic flow of  $M=1.6234$  and a wave angle  $\alpha = 28.94^\circ$ , the deflection angle  $\beta$  is less than  $2^\circ$  which is much lower than  $\beta=9.492^\circ$  as observed in Fig.11. From the above facts it is thus concluded that the wave denoted by AC in Fig.11 is not a projection of the acoustic wave inside the cavity. This wave experiences an effective flow deflection angle  $\beta$  that is less than that of the shear layer deflection angle.

Flow phenomena associated with the narrowest cavity with  $L/W=4$  is similar to the other two cavities though the disturbances created in the main flow and the shear layer structure are different from them. This is evident from the images obtained from shadowgraph visualization for this cavity which is shown in Fig.12(a)-(c). As the shear layer comes out of the cavity near the trailing edge, large scale structures are observed in the freestream for the wider cavities as seen in Figs. 9(c) and 10(b). The structures marked as 7 in Fig.12 are not as prominent and large for the narrowest cavity which also shows an imprint of the trailing edge bow shock. This is indicative of the shear layer fluctuating at a different rate than the other two cavities.

Vortex roll up and waves generated due to deflection of shear layer are observed for the narrowest cavity and is marked as 5 and 8 respectively in Fig.12. Overall, the flow in the mainstream in the vicinity of the narrowest cavity is observed to be quieter as compared to the



wider cavities. The roll up vortices forming the shear layer is seen to be confined to a narrow region along the cavity lip of all the three models which moves along the length of the cavity to the trailing edge wall. Overall, not much activity is visible inside the cavity except at the trailing edge for the cavities with  $L/W=2$  and 3.

Instantaneous shadowgraph images for the 2D cavity model are shown in Fig.13. Deflection of the shear layer into the cavity and subsequent exposure of the trailing edge to the supersonic mainstream flow generating a bow shock at the trailing edge of the cavity is marked as 3 in Fig.13(a). Features similar to the other models are observed for this case also and the different flow and wave structures are marked according to the previous cases as shown in Fig.13(a)-(d). Vigorous interaction of the shear layer with the trailing edge was observed as in the case of the wider 3D cavities and is indicated as 7.

#### 4. CONCLUSIONS

The wave and shear layer structure in a supersonic flow of Mach number 1.7 over 3D wall mounted cavities located in a rectangular duct are investigated experimentally. Comparison between 3D cavities and a nominal 2D cavity is also undertaken in the study. Time averaged flow visualization shows the details of shock structure formed due to the presence of unstable shear layer along the length of the cavity. Insight into the mechanism of quasi steady shock formation, propagation of acoustic wave inside cavity and the unsteady shear layer structure are provided by

instantaneous flow visualization. Disturbances induced in the mainstream by the widest 3D cavity are observed to be much higher than the other models. For the case of the narrowest cavity model,  $L/W=4$  the mainstream flow is observed to be much quieter than the wider cavities. A thicker shear layer at the leading edge for the widest 3D cavity ( $L/W=2$ ) generates a relatively stronger oblique shock in the mainstream and the associated higher total pressure losses.

#### REFERENCES

- 1) Henderson, J., Babcock, K.J., and Richards, B.E.: Understanding Subsonic and Transonic Cavity Flows, *Aeronautical J.*, Vol. 105, No. 1044(2001), 77-84.
- 2) Rockwell, D. and Naudascher, E.: Review- Self Sustaining Oscillations of Flow past Cavities, *J. of Fluids Engineering*, Vol. 100, No. 6, June (1978), 152-165.
- 3) Zhang, X.: Compressible Cavity Flow Oscillation Due to Shear Layer Instabilities and Pressure Feedback, *AIAA J.*, Vol. 33, No. 8 (1995), 1404-1411.
- 4) Heller, H., and Delfs, J.: Cavity Pressure Oscillations: the Generating Mechanism Visualized, *J. of Sound and Vibration*, No- 196(2) (1996), 248-252.
- 5) Rona, A., Zhang, X. and Edwards, J.A: An Observation of Pressure Waves around a Shallow Cavity, *J. of Sound and Vibration*, No- 214(4) (1998), 771-778.